DTU Library

A Combined TheoryExperiment Analysis of the Surface Species in LithiumMediated NH3 Electrosynthesis

Schwalbe, Jay A.; Statt, Michael J.; Chosy, Cullen; Singh, Aayush R.; Rohr, Brian A.; Nielander, Adam C.; Andersen, Suzanne Zamany; McEnaney, Joshua M.; Baker, Jon G.; Jaramillo, Thomas F.

Total number of authors:
12

Document Version
Peer reviewed version

Link back to DTU Orbit

Accepted Article

Title: A Combined Theory-Experiment analysis of the Surface Species in Lithium Mediated NH3 Electrosynthesis

Authors: Jay A. Schwalbe, Michael J. Statt, Cullen Chosy, Aayush R. Singh, Brian A. Rohr, Adam C. Nielander, Suzanne Z. Andersen, Joshua M. McEnaney, Jon G. Baker, Thomas F. Jaramillo, Jens K. Norskov, and Matteo Cargnello

This manuscript has been accepted after peer review and appears as an Accepted Article online prior to editing, proofing, and formal publication of the final Version of Record (VoR). This work is currently citable by using the Digital Object Identifier (DOI) given below. The VoR will be published online in Early View as soon as possible and may be different to this Accepted Article as a result of editing. Readers should obtain the VoR from the journal website shown below when it is published to ensure accuracy of information. The authors are responsible for the content of this Accepted Article.

A Combined Theory-Experiment analysis of the Surface Species in Lithium-Mediated NH₃ Electrosynthesis

Dr. Jay A. Schwalbe [a], Michael J. Statt [a], Cullen Chosy [a], Dr. Aayush R. Singh [a], Brian A. Rohr [a], Dr. Adam C. Nielander [a], Suzanne Z. Andersen [b], Dr. Joshua M. McEnaney [a], Jon G. Baker [a], Prof. Thomas F. Jaramillo [a], Prof. Jens K. Norskov [*b], Prof. Matteo Cargnello [*a]

[a] Department of Chemical Engineering and SUNCAT Center for Interface Science and Catalysis,

Stanford University, Stanford, CA 94305, USA

[b] Department of Physics, Technical University of Denmark, Kongens Lyngby, Denmark

[*]Corresponding authors: mcargnello@stanford.edu (M.C.); jkno@dtu.edu (J. K. N.)

Abstract

Electrochemical processes for ammonia synthesis could potentially replace the high temperature and pressure conditions of the Haber-Bosch process with voltage, offering a pathway to distributed fertilizer production that leverages the rapidly decreasing cost of renewable electricity. However, nitrogen is an unreactive molecule and the hydrogen evolution reaction (HER) presents a major selectivity challenge. An electrode of electrodeposited lithium in tetrahydrofuran solvent overcomes both problems by providing a surface that easily reacts with nitrogen and by limiting the access of protons with a nonaqueous electrolyte. Under these conditions, we measure relatively high faradaic efficiencies (~10%) and rates (0.1 mA cm^{-2}) toward NH₃. We observe development of a solid electrolyte interface (SEI) layer as well as the accumulation of lithium and lithium-containing species. Detailed DFT studies suggest lithium nitride and hydride to be catalytically active phases given their thermodynamic and kinetic stability relative to metallic lithium under reaction conditions and the fast diffusion of nitrogen in lithium.

Introduction

The electrochemical synthesis of fuels and commodity chemicals is a promising way to leverage the rise of inexpensive, renewable electricity. Interest in the electrochemical nitrogen reduction reaction (NRR) is driven by the opportunity to convert electricity from renewable sources into ammonia, a key component of synthetic fertilizers.[1] Currently, ammonia is produced in centralized chemical facilities using the Haber-Bosch process, the thermal reaction between nitrogen and hydrogen at high temperatures and pressures. This process consumes large amounts of natural gas for the production of hydrogen resulting in the emission of large quantities of greenhouse gases.[2] There are many routes that have been explored to replace fossil fuels with electricity as the energy input. Plasma processes (based on arc-discharge) pre-date the Haber-Bosch process and can turn air directly into NO_x species.[3] The Haber-Bosch process can be powered with electricity via water electrolysis-derived H_2, but still requires high pressures and temperatures.[4] Chemical or electrochemical looping strategies have been shown to provide high selectivity to ammonia;[5,6] their implementation and operation still need to be verified. All these strategies require temperatures or pressures above ambient. An electrocatalytic approach is a strategy to avoid these harsh operating conditions by using the reducing potential of protons and electrons to drive the reaction.
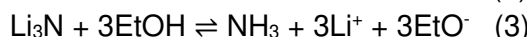
The numerous challenges faced by researchers in this field are well documented.[7] The first barrier is the reliable detection of small amounts of ammonia typically produced during the electrochemical experiments. While some recent investigations of NRR have shown faradaic efficiencies that exceed 10%, historically electrochemical systems have shown faradaic efficiencies (FE) to ammonia below 1% and low reaction rates, presenting a challenge to collecting reliable data because common sources of fixed nitrogen contamination occur at similar levels. It is therefore crucial that measurements are taken with extraordinary rigor in order to clearly verify the ammonia synthesis from N_2, and even then there are many possible sources of error.[8] These low rates also limit the applications of electrochemical ammonia synthesis, as rates on the order of 0.1 A cm^{-2} (or higher) are the target for other industrial applications of electrochemistry, orders of magnitude greater than what has been measured for NRR.[9,10]

A fundamental challenge to efficient electrocatalytic NRR is the competing hydrogen evolution reaction (HER).[11] At the reducing potentials required to drive ammonia synthesis, H_2 can also be formed. Many efforts have been made to overcome this challenge by finding an active and selective catalyst.[12] Some groups have reported that catalysts such as gold, which binds protons too weakly for high HER activity, can selectively make ammonia.[13] However, the high activation barriers and low rates observed for gold exemplify the difficulty of making reliable NH_3 measurements. Transition metal nitrides have been predicted to have active sites that are selective to N_2 activation over hydrogen production.[14] Unfortunately, they have been shown experimentally to suffer from the same selectivity issues in aqueous environments because of potential reconstructions or to be potentially unstable.[15] A recent critical exploration of some nitrides also highlighted the need to consider the contribution of lattice nitrogen to apparent ammonia synthesis.[16]

Recently, we proposed models that demonstrated how the large availability of protons in aqueous systems is the main reason why selectivity to NRR is so low.[17,18] Following this model, we herein focus on non-aqueous electrolytes, where the activity of protons can be controlled

2

independently of catalyst surface by operating at a low proton concentration. A number of such systems have been described and are generally able to achieve faradaic efficiencies in excess of 10% and have been subjected to rigorous control experiments that make them reliable and reproducible.[19,20] In this work, we investigate the details of ammonia synthesis on electrodeposited lithium in tetrahydrofuran (Li-THF). This system has recently received renewed attention due to its rigorous verification and high absolute performance.[20,21]

The mechanism for ammonia synthesis in the Li-THF system is summarized in equations 1-3. First, lithium is reduced from solution (step 1), next it reacts with nitrogen to form lithium nitride (step 2), and finally lithium nitride reacts with ethanol to yield ammonia (step 3):[20,21]

$$Li^+ + e^- \rightleftharpoons Li \qquad\qquad\qquad (1)$$
$$6Li + N_2 \rightleftharpoons 2Li_3N \qquad\qquad\qquad (2)$$
$$Li_3N + 3EtOH \rightleftharpoons NH_3 + 3Li^+ + 3EtO^- \quad (3)$$

The individual protonation steps (i.e. NH to NH$_2$) are fast and the reaction of lithium with nitrogen is the rate determining step for NRR.[20] Ethanol is chosen as the proton source due to its high performance in early studies.[21] Open questions remain regarding the details of the mechanism along with identifying the active site for nitrogen activation. Previous reports of this system consider lithium metal as well as lithium nitride as intermediates, which are fully dissolved during the formation of ammonia.[21] This implies that N$_2$ is activated on nascent lithium clusters, forming a local cycling of lithium (Figure 1a). However, our electrochemical characterization shows the development of a long-lived layer of lithium metal with the additional formation of other SEI species. This discovery motivated an investigation of a possible heterogeneous catalytic cycle. Thermodynamic analysis suggests that deposited lithium will react to form lithium nitride and lithium hydride under reaction conditions. DFT calculations show that there are favorable pathways for ammonia synthesis on the surface of all three species (Li, LiH, Li$_3$N) at the potentials applied. Therefore, we propose that a more complex reaction mechanism is at play. Beyond freshly plated lithium, nitrogen activation and ammonia synthesis can proceed over other stable surfaces as well (Figure 1b).
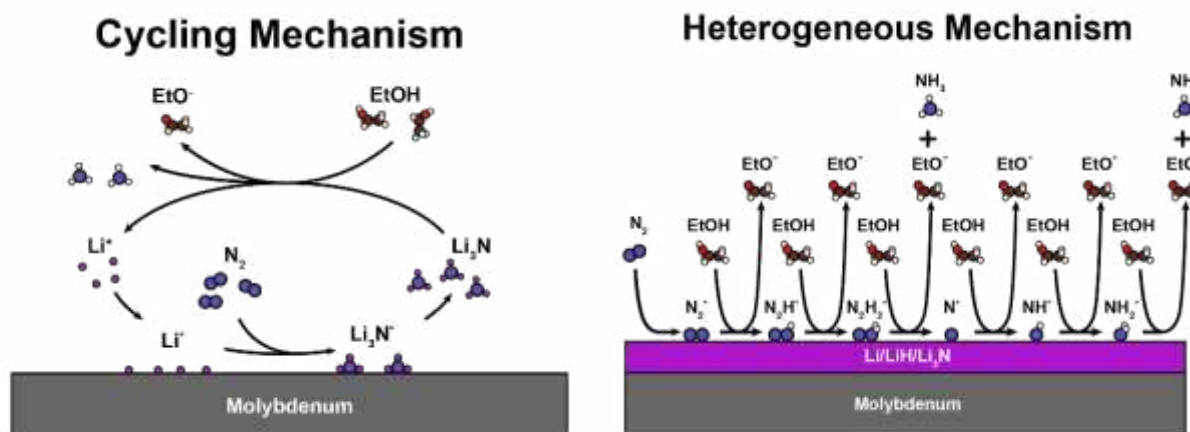
Figure 1. a) a sketch of the 'cyclic mechanism' in which lithium atoms are only transiently on the surface. b) a 'Heterogeneous mechanism', in which there is a stable amount of lithium on the electrode at all times.

Results and Discussion

Electrochemical Characterization

Figure 2a shows cyclic voltammograms of a molybdenum cathode in tetrahydrofuran-ethanol electrolytes. The plating and stripping of lithium are identifiable at -3.8 V vs. Ag/Ag+ at all three levels of added ethanol. This feature shows that lithium can be reduced and is stable on the electrode even with a considerable concentration of protons in solution. The reduction peak between -2 and -3 V vs. Ag/Ag+ varied prominently with the amount of ethanol added. Therefore, we conclude that this feature is the reduction of protons derived from ethanol to produce hydrogen. This conclusion is further supported by previous reports that demonstrate that HER in pure ethanol occurs in a very similar potential window (Supporting Information Figure S2).[22] The reduction current observed even in the absence of added ethanol is likely related to lithium underpotential deposition and SEI formation, following literature reports.[23] The anodic stripping feature on the positive sweep at -2 V vs. Ag/Ag+ decreases with increasing ethanol concentration, suggesting that the lithium is indeed reacting with ethanol. Further evidence of a strong interaction between ethanol and the surface is shown in the scan at 5% ethanol, which shows a lower plating and stripping current.
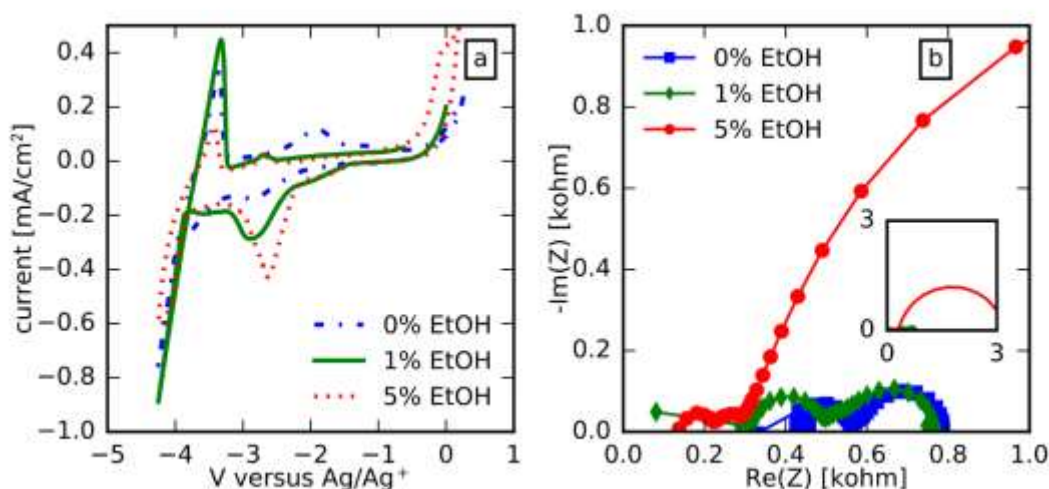
Figure 2. Electrochemical measurements of a molybdenum working electrode in 0.5 M LiClO$_4$ in tetrahydrofuran with various amounts of ethanol added (0, 1 or 5 vol. %). (a) cyclic voltammetry at a scan rate of 10 mV/s. Nitrogen gas was supplied in all experiments, the scan shown is the third one. (b) Electrochemical Impedance Spectroscopy (EIS) at open circuit voltage at various ethanol concentrations after 30 minutes of electrolysis. Inset shows a larger range of impedance data.

Motivated by the cyclic voltammetry, we investigated the formation of an SEI layer in this system using electrochemical impedance spectroscopy (EIS). As with most organic electrolytes at very reducing potentials, either the solvent, supporting electrolyte, or impurities are likely to decompose at the electrode. Figure 2b shows the impedance spectroscopy of the same electrolytes as in Figure 2a. We observed two depressed semicircular features which are typical of a fast surface reaction and a slower diffusion process through a nascent SEI layer.[24] The depressed semi-circular, low-frequency loop suggests the presence of a rough surface with a layered structure.[24] The EIS behavior stabilizes after 30 minutes and remains steady over at least 2 hours (Figure S3). Interestingly, the electrode with 5 vol. % ethanol rapidly developed a high impedance, low-frequency loop. This behavior suggests that the ethanol passivates the electrode at high concentrations, thus modifying the formation of the SEI layer and reducing the deposition of lithium on the surface, consistent with the reduced lithium stripping feature in the anodic scan in Figure 1a at 5 vol. % ethanol. Similarly, when the system is not stirred (Figure S3), the low-frequency loop develops higher impedance in the presence of ethanol, even at 0.5 vol. %, than when ethanol is absent. This behavior would be expected in any system with possible mass transport limitations. However, if this behavior were related to depletion of ethanol as a reactant, then the impedance should not be greater than that of the case when ethanol is absent. Rather than depletion of reactant, it may instead be caused by build-up of the product, ethoxide. This observation also agrees with the decreased lithium plating current seen in the cyclic voltammetry at 5 vol. % ethanol. CV and EIS experiments therefore suggest that a balance of lithium deposition, SEI formation and reactions with solvent are important to determine the active state of the surface to produce ammonia.

Ammonia synthesis results and time-dependent behavior

We investigated the current density dependence of the ammonia synthesis rate and faradaic efficiency in a solution of tetrahydrofuran with 1 vol. % added ethanol. Due to the high solution resistance and possible drift of the pseudo-reference, constant current measurements were typically more stable than constant voltage experiments. The ammonia synthesis in the Li-THF system has been subjected to rigorous verification (specifically isotopically labelled nitrogen experiments with appropriate gas purification) by multiple efforts previously, including our own.[7,20] For this work, we performed the control experiments necessary to ensure that our experimental set-up was free from any contamination: nitrogen purge at open circuit voltage to test for direct ammonia contamination of the nitrogen feed; Ar purge with applied voltage to test for contamination from the cell; and time-resolved measurements showed linear accumulation of ammonia (Figure S4, Figure 3c). The amount of ammonia observed in the absence of nitrogen purge or applied voltage was too small to be quantified while typical experimental results contained 100 µM or greater as measured by ^{1}H-NMR. The range of currents investigated here is similar to that considered by researchers in earlier work,[21] but below that used in more recent work.[20] For extended chronopotentiometry experiments we selected a current density of 1.1 mA cm^{-2} because it showed a stable voltage over time.

Both the absolute rate and the faradaic efficiency of ammonia synthesis increased as a function of total applied current density up to values of 0.08 mA cm^{-2} and ~10%, respectively, measured at a total current density of 0.8 mA cm^{-2} (Figure 3a). After this point, the absolute rate

5

of ammonia synthesis remained constant within error at approximately 0.1 mA cm^{-2} even upon increasing the total current density up to 3.3 mA cm^{-2}, with a commensurate decrease in faradaic efficiency. The trend in ammonia current with total current could be explained by either the number of active sites increasing with current and then leveling off, or with increasing activity of a constant number of active sites. Representative chronopotentiograms are shown in Figure 3b. While the voltage varies over the course of the experiments, it does not diverge and tends to stabilize towards the end of each experimental run. Note that the applied voltage is much greater than the onset of proton reduction observed in Figure 2a at -2V. In Figure S5 we compare the relationship between i_{NH3} and i_{total} to what has been reported in reference 20. While our observations are qualitatively the same, they are quantitatively different and we extract a different slope in the log-log plot of i_{NH3} versus i_{total} (0.88 in this work compared to 1.60 in previous work). This reaction is sensitive to a variety of experimental conditions, as shown here and in the literature. We note here that our purge rate is much lower (2 mL min^{-1} versus 10 mL min^{-1}) and the ethanol concentration is lower than in reference 20.
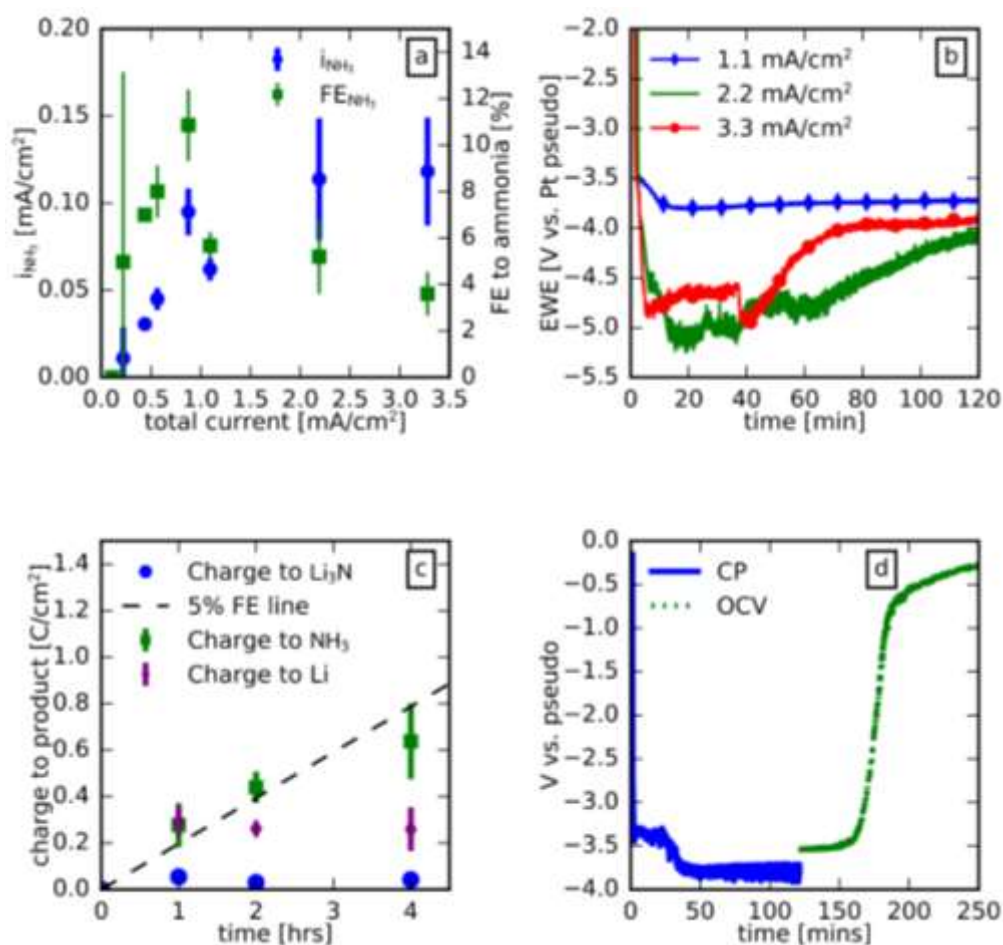

Figure 3. Ammonia synthesis results for a 1 vol. % ethanol in tetrahydrofuran with 0.5 M LiClO$_4$ supporting electrolyte. Nitrogen gas was supplied at a rate of 2 mL min^{-1}. Error bars represent the standard deviation of at least three measurements. (a) Partial current density to ammonia (i_{NH3}, left y-axis) and faradaic efficiency to ammonia (FE$_{NH3}$, right y-axis) as a function of total applied current. All experiments were performed for 2 hours. (b) Chronopotentiograms for representative

experiments plotted in panel (a). Voltages are reported versus platinum pseudo-reference. (c) Time-resolved accumulation of ammonia, lithium, and apparent fixed nitrogen on the surface after electrolysis at 1.1 mA cm^{-2} for 1, 2 and 4 hours. Each point is an independent experimental run. Error bars are the standard deviation of three measurements. (d) Two hour chronopotentiogram (CP) at 1.1 mA cm^{-2} followed by the relaxation of the open circuit voltage (OCV).

Figure 3c shows the time evolution of ammonia, along with the build-up of both nitrogen containing species and lithium on the electrode surface, as measured for a current density of 1.1 mA cm^{-2}. Ammonia was accumulated over a 4 hour experimental run, in line with previous results. The fixed nitrogen was mainly ammonia. As lithium nitride has been implicated as an intermediate in this process, we attempted to detect it in the deposited material on the working electrode. After an experiment, the cathode was removed from the electrochemical cell and immersed in 1.5 mL of water. Any lithium nitride on the cathode would be hydrolyzed to ammonia as expected from previous work.[5] The amount of ammonia following hydrolysis was then quantified. It is also possible that nitrogen was fixed on the electrode as lithium amide or lithium imide. Assuming a stoichiometry of three electrons per nitrogen, the charge towards lithium-nitrogen species was relatively constant at 0.05 C/cm^2. We also note that due to the many sources of contamination, this should be treated as an upper bound on the amount of fixed nitrogen. A more direct measure of the speciation of the fixed nitrogen on the electrode would require in-situ spectroscopic measurements, as the lithium surface is extremely sensitive to air. To quantify the amount of electrochemically connected lithium on the electrode, the deposited material was stripped off under an oxidizing potential (Figure S7). These amounts are plotted in Figure 3c as the charge towards lithium. Initially, a large fraction of the current went to lithium deposition. The surface appears to reach steady-state within one hour. We used the same technique to measure the relationship between electrochemically connected lithium on the surface, total current, and current to ammonia, shown in Figure S3.

Considering the visual accumulation of species on the electrode (Figure S6), as well as the evidence of deposited lithium in the cyclic voltammetry experiments, we investigated open circuit voltage (OCV) of the electrode after ammonia synthesis. We observed that the OCV value was stable at roughly the potential observed for Li/Li$^+$. Second, as shown in Figure 3d, after a 2 hour hold at constant current the OCV was stable for a period of roughly 30 minutes and then decayed smoothly. This observation suggests that under these reaction conditions the surface had a high coverage of lithium and that there was a mechanically and chemically long-lived amount of material deposited on the electrode. The voltage was slightly positive of the observed lithium plating potential in Figure 2a, as is to be expected for a metal surface that is corroding. Other species, such as lithium nitride or lithium amide, may be expected to play a role in the surface equilibrium if they are in electrical contact with the electrode. The lack of a second voltage plateau is weak evidence that these species do not play a major role, as they could simply have lost contact with the electrode as the lithium corroded or have slow dissolution kinetics.

DFT studies

From the experimental characterization, we conclude that the electrode surface contains significant amounts of reduced lithium metal during ammonia production. Therefore, it is useful to

7

understand how a surface of lithium-containing materials can act as a heterogenous catalyst for the NRR and their thermodynamic and kinetic stabilities. We turn to theory to probe the candidate surfaces and investigate three criteria. First, what thermodynamics tells us is possible given a nitrogen-lithium-hydrogen system. Second, which surfaces are active enough to reduce nitrogen to ammonia at these conditions. Lastly, which are kinetically stable under operating conditions.

The bulk phase stability indicates that there is a large driving force for lithium metal to react to form both lithium hydride (LiH) and lithium nitride (Li_3N) in the presence of protons and nitrogen (Table 1). Additionally, the kinetics of these two reactions are facile, as evidenced by Li_3N formation at room temperature.[5] This result is due to the low diffusion barriers for nitrogen in lithium and lithium/nitrogen vacancies in Li_3N (Figure S8). Therefore, we can conclude that there is a significant thermodynamic driving force for a reduced lithium surface to transform into the hydride or nitride phase under reaction conditions. It is possible that mixed $Li_xN_yH_z$ species, such as lithium imide (Li_2NH) and lithium amide ($LiNH_2$), exist on the surface. In fact, NH and NH_2 species must be formed in the course of producing ammonia by protonating nitrogen. However, these surfaces are considerably more complicated to model as they are lower order systems with significantly more potential crystal structures, facets, and surface terminations. Characterizing and modeling the mixed $Li_xN_yH_z$ species is an important step towards understanding lithium-mediated ammonia synthesis but is beyond the scope of this work. Additionally, understanding how pure Li_3N and LiH interact with NRR intermediates will help guide and contextualize how mixing these phases may impact catalytic activity. Therefore, NH and NH_2 species are considered only as surface intermediates in the limiting potential analysis conducted below.

Table 1. Summary of thermodynamic quantities for given reactions involving lithium-containing species relevant for the reaction conditions used in this work.[25] SHE represents the standard hydrogen electrode.

Chemical Reaction	ΔG(0 V vs SHE)	ΔG(-3 V vs SHE)
½ N_2 + 3Li ⇔ Li_3N	-1.70 eV	-1.70 eV
(H^++e^-) + Li ⇔ LiH	-0.94 eV	-3.94 eV
Li_3N + 3(H^++e^-) ⇔ 3Li + NH_3	+1.06 eV	-7.94 eV

We used DFT calculations and limiting potential analysis to assess the electrochemical NRR pathway on lithium, lithium nitride, and lithium hydride surfaces. This will be relevant to lithium electrochemically connected to the electrode, and to disconnected lithium where the dissolution is driven by the loss of lithium metal to lithium ions. Lithium is chosen because the experimental data shows that only a small amount of the lithium that is plated reacts to form a nitrogen-containing species. The nitride and hydride are chosen on the basis of the thermodynamic argument presented above. Shown in Figure 4, we find that plausible pathways exist on all three surface species. For the nitride and hydride, the active site is a vacancy, in line with other work on nitride materials.[14,26] The required limiting potential for ammonia formation on

8

lithium, lithium nitride, and lithium hydride surfaces is -0.76 V, -1.33 V, -1.53 V vs RHE, respectively. All pathways go through absorbed NH_x intermediates. However, these intermediates are ultimately able to be reduced to ammonia. It is important to note that assumptions of the computational hydrogen electrode (CHE) are present in the analysis of the limiting potential.[27] The CHE assumes an aqueous electrolyte, where pH is well defined. To account for the non-aqueous electrolyte present in this experiment, we used the onset potential for ethanol reduction from the experiments shown in Figure 2a as a benchmark. The data indicates that all three surfaces are active towards ammonia synthesis at the operating conditions of these experiments.
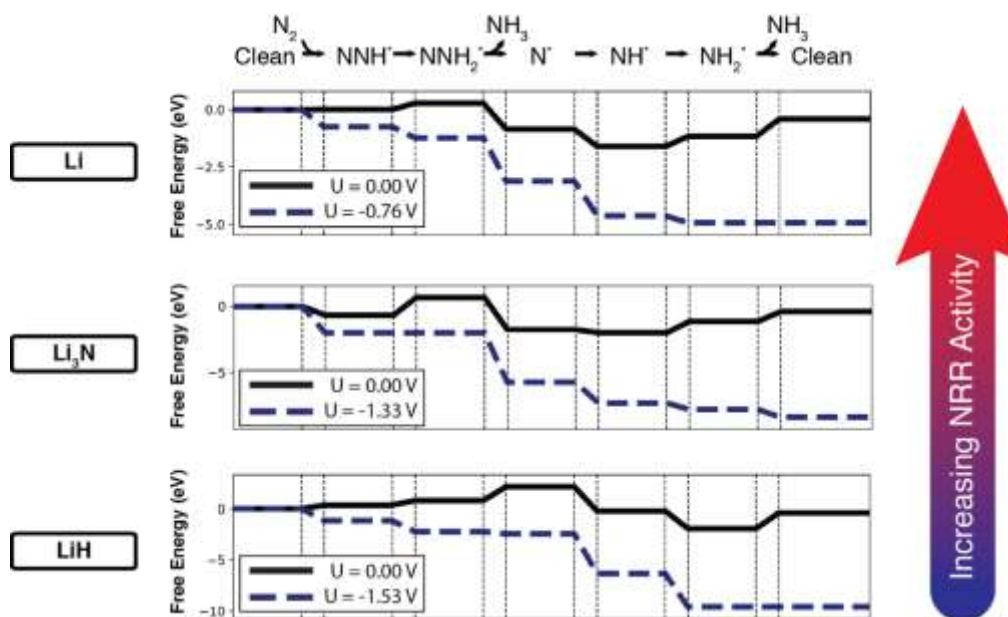

Figure 4. Free energy diagrams for NRR on Li, Li_3N, and LiH. The mechanisms were carried out in the long-bridge site, the nitrogen vacancy site, and the hydrogen vacancy site for Li, Li_3N, and LiH, respectively (for further details see Figure S9). The dashed line shows the free energy diagram when the limiting potential is applied (i.e. the potential required to make steps exergonic). All three surfaces are predicted to be catalytically active toward ammonia synthesis at the potentials of lithium plating.

To assess the final criteria, we must also consider the stability of each phase under large reducing potentials. As shown in line 3 of Table 1, Li_3N can decompose into lithium and ammonia in the presence of protons when a sufficiently large reducing potential is applied. The potential dependence of this decomposition leads to an extraordinarily large driving force at the experimental operating conditions. This analysis suggests that while Li_3N may be stable relative to lithium and nitrogen in isolation, if a proton source is present, Li_3N becomes thermodynamically unstable and decomposes into ammonia and lithium metal. This conclusion is essentially that of the original experiments of Tsuneto *et al.,* that lithium nitride is such an unstable species relative to ammonia that it should rapidly decompose.[21] However, one must consider the kinetics of decomposition, particularly important here as the decomposition mechanism could entail a combination of electrochemical and chemical steps. The large driving force of the decomposition process results from the relatively large potential-dependence of the reaction. The kinetics scale

9

with the applied potential only up until the point at which all electrochemical reaction barriers are brought lower than the largest chemical barrier to decomposition. After that point, the largest chemical barrier determines the rate of decomposition. Thus, if a large chemical barrier is encountered along the decomposition pathway, lithium nitride could be kinetically stable.

Our calculations reveal a possible bottleneck to decomposition: the diffusion of vacancies from the bulk to the surface. Since a surface vacancy is the active catalytic site for both nitrides and hydrides, a significant presence of surface vacancies is required for active catalysts. If a vacancy is more stable at the surface of the material than in the bulk, then the vacancy will remain at the surface producing hydrogen and ammonia. If the vacancy is more stable in the bulk than at the surface, the vacancy will have a driving force to move into the bulk, eliminating the active site as fresh lattice nitrogen or hydrogen is brought to the surface to fill the vacancy. Thus, stable surface vacancies relative to bulk vacancies should correlate with a chemical barrier to decomposition, providing a kinetic stability that may stabilize even thermodynamically unstable materials, such as Li_3N. Figure 5 shows that lithium nitride has a stable surface nitride vacancy relative to a bulk nitride vacancy. This observation, along with the fact that bulk lithium nitride is stable relative to bulk lithium metal, indicates that adsorbed nitrogen will tend to fully convert metallic lithium to the nitride phase. In comparison, lithium hydride has an unstable surface vacancy, essentially providing facile kinetics for lattice hydrogen to reach the surface. However, since lithium hydride is also thermodynamically stable at these operating conditions, decomposition should not occur. Therefore, even though lithium is an active NRR catalyst, some amount of adsorbed nitrogen and hydrogen will diffuse into lithium over time, forming thicker nitride and hydride layers. Lithium hydride is thermodynamically stable, while lithium nitride is kinetically stable. This picture is consistent with small amounts of Li-N species on the electrode at the end of experiments. The experimental techniques employed here cannot detect lithium hydride. The surface reached, to our ability to observe, a stable state within one hour. This observation suggests that either due to conductivity or to depletion of lithium, lithium plating slows over the course of the experiments. However, from a thermodynamic and stability analysis, the hydride and nitride are able to continue to form throughout the experiment. Since the ammonia production also is relatively constant, it suggests that the active catalytic surface is unperturbed throughout the experiment. It is concluded that at steady state operating conditions, the catalytic surface will ultimately be a combination of lithium nitride and lithium hydride.
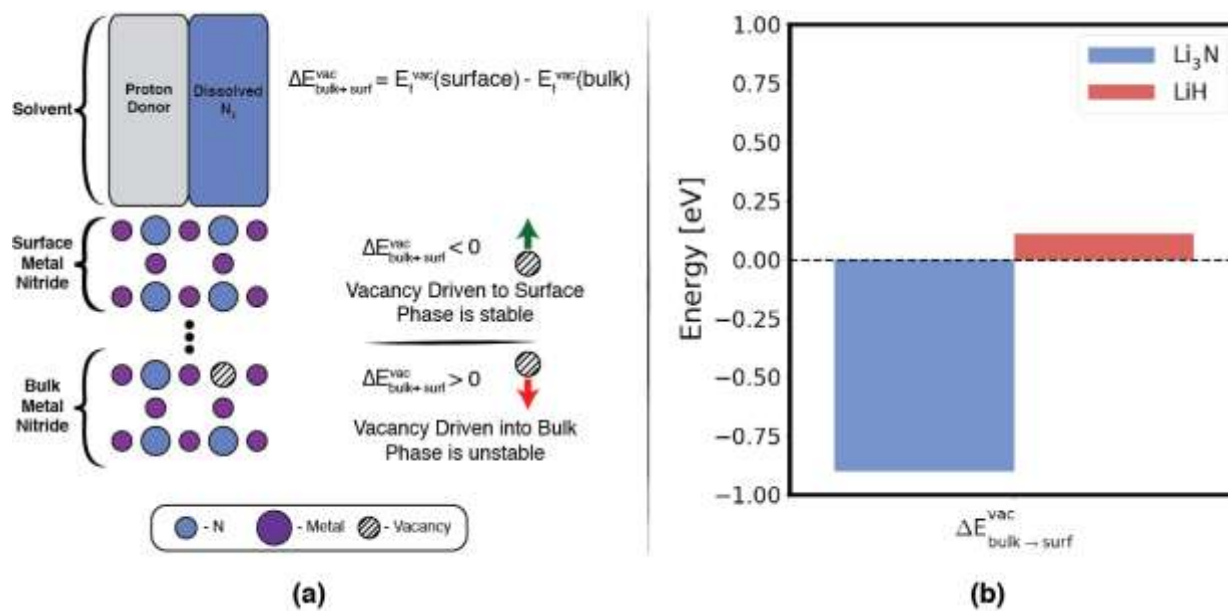
Figure 5. (a) A schematic defining the driving force acting on a bulk nitrogen vacancy within a nitride. If the driving force is negative, the bulk vacancy would be driven to the surface. If positive, the surface vacancies would be driven to the bulk. (b) Lithium nitride has the property of having stable surface vacancies, which likely relates to their rapid nitridation as well as potential catalytic activity.

Based on this thermodynamic analysis we propose that ammonia synthesis in the Li-THF system proceeds through an associative mechanism on either a lithium nitride or hydride surface as shown in Figure 1b. This conclusion accounts for our experimental observation of large amounts of lithium on the surface of the electrode at the end of electrolysis. However, it does not account for the increase in ammonia synthesis rate with total current. One possibility is that there are non-zero electrochemical barriers in the mechanism and therefore each active site has a voltage-dependent activity. This result could take the form of a low barrier for a proton transfer step or a non-negligible coverage of ethoxide anions on the surface that need to be removed. The other explanation is that the electrochemically active surface area changes with current, but that the activity per surface area is constant. The simplest possibility is that the deposited lithium has a constant surface area per mass. Indeed, the amount of lithium stripped from the electrode correlates to the total current passed ($C_{Li} \sim i^{0.45}$). However, the rate of ammonia synthesis is not proportional to the observed amount of lithium stripped ($i_{NH3} \sim C_{Li}^{1.6}$). This observation suggests that a combination of effects is responsible for the results in Figure 3a.

Conclusions

The THF-ethanol electrolyte system allows for reduced access of protons to the active site and the stabilization of highly reactive lithium surfaces. These two factors allow for relatively efficient ammonia synthesis. In the regime that we investigated here, we describe the complexities of the surface, combining experimental and computational approaches. Electrochemical characterization of the system shows potential influence of a solid electrolyte interphase layer and

11

accumulation of lithium and related species on the surface. Density functional theory calculations support this observation. Theory predicts that lithium, lithium nitride, and lithium hydride can produce ammonia under the experimental conditions. The free energy landscape also shows that mixed lithium-nitrogen-hydrogen species are likely intermediates in the process. These results will help guide future *in-situ* studies to directly identify the active species and motivate further research into materials beyond lithium that may be able to similarly activate nitrogen and form ammonia electrochemically.

Acknowledgements

References

[1] B. H. R. Suryanto, H.-L. Du, D. Wang, J. Chen, A. N. Simonov, D. R. MacFarlane, *Nat. Catal.* **2019**, *2*, 290.
[2] J. G. Chen, R. M. Crooks, L. C. Seefeldt, K. L. Bren, R. M. Bullock, M. Y. Darensbourg, P. L. Holland, B. Hoffman, M. J. Janik, A. K. Jones, et al., *Science* **2018**, *360*, eaar6611.
[3] N. Cherkasov, A. O. Ibhadon, P. Fitzpatrick, *Chem. Eng. Process. Process Intensif.* **2015**, *90*, 24–33.
[4] E. Cussler, A. McCormick, M. Reese, M. Malmali, *JoVE J. Vis. Exp.* **2017**, e55691.
[5] J. M. McEnaney, A. R. Singh, J. A. Schwalbe, J. Kibsgaard, J. C. Lin, M. Cargnello, T. F. Jaramillo, J. K. Nørskov, *Energy Environ. Sci.* **2017**, *10*, 1621–1630.
[6] R. Michalsky, A. M. Avram, B. A. Peterson, P. H. Pfromm, A. A. Peterson, *Chem. Sci.* **2015**, *6*, 3965–3974.
[7] S. Z. Andersen, V. Čolić, S. Yang, J. A. Schwalbe, A. C. Nielander, J. M. McEnaney, K. Enemark-Rasmussen, J. G. Baker, A. R. Singh, B. A. Rohr, et al., *Nature* **2019**, 1.
[8] L. F. Greenlee, J. N. Renner, S. L. Foster, *ACS Catal.* **2018**, *8*, 7820–7827.
[9] J. M. Spurgeon, B. Kumar, *Energy Environ. Sci.* **2018**, *11*, 1536–1551.
[10] M. R. Shaner, H. A. Atwater, N. S. Lewis, E. W. McFarland, *Energy Environ. Sci.* **2016**, *9*, 2354–2371.
[11] J. H. Montoya, C. Tsai, A. Vojvodic, J. K. Nørskov, *ChemSusChem* **2015**, *8*, 2180–2186.
[12] X. Zhu, S. Mou, Q. Peng, Q. Liu, Y. Luo, G. Chen, S. Gao, X. Sun, *J. Mater. Chem. A* **2019**, DOI 10.1039/C9TA13044F.
[13] D. Bao, Q. Zhang, F.-L. Meng, H.-X. Zhong, M.-M. Shi, Y. Zhang, J.-M. Yan, Q. Jiang, X.-B. Zhang, *Adv. Mater.* **2017**, *29*, 1604799.
[14] Y. Abghoui, E. Skúlason, *Catal. Today* **2017**, *286*, 78–84.
[15] X. Yang, J. Nash, J. Anibal, M. Dunwell, S. Kattel, E. Stavitski, K. Attenkofer, J. G. Chen, Y. Yan, B. Xu, *J. Am. Chem. Soc.* **2018**, *140*, 13387–13391.
[16] H.-L. Du, T. R. Gengenbach, R. Hodgetts, D. R. MacFarlane, A. N. Simonov, *ACS Sustain. Chem. Eng.* **2019**, *7*, 6839–6850.
[17] A. R. Singh, B. A. Rohr, J. A. Schwalbe, M. Cargnello, K. Chan, T. F. Jaramillo, I. Chorkendorff, J. K. Nørskov, *ACS Catal.* **2017**, *7*, 706–709.
[18] A. R. Singh, B. A. Rohr, M. J. Statt, J. A. Schwalbe, M. Cargnello, J. K. Nørskov, *ACS Catal.* **2019**, 8316–8324.

[19] F. Zhou, L. M. Azofra, M. Ali, M. Kar, A. N. Simonov, C. McDonnell-Worth, C. Sun, X. Zhang, D. R. MacFarlane, *Energy Environ. Sci.* **2017**, *10*, 2516–2520.

[20] N. Lazouski, Z. J. Schiffer, K. Williams, K. Manthiram, *Joule* **2019**, *3*, 1127–1139.

[21] A. Tsuneto, A. Kudo, T. Sakata, *J. Electroanal. Chem.* **1994**, *367*, 183–188.

[22] A. A. Inocencio, *Electrochimica Acta* **1978**, *23*, 977–981.

[23] D. Aurbach, M. Daroux, P. Faguy, E. Yeager, *J. Electroanal. Chem. Interfacial Electrochem.* **1991**, *297*, 225–244.

[24] A. Zaban, E. Zinigrad, D. Aurbach, *J. Phys. Chem.* **1996**, *100*, 3089–3101.

[25] A. Jain, S. P. Ong, G. Hautier, W. Chen, W. D. Richards, S. Dacek, S. Cholia, D. Gunter, D. Skinner, G. Ceder, et al., *APL Mater.* **2013**, *1*, 011002.

[26] X. Yang, S. Kattel, J. Nash, X. Chang, J. H. Lee, Y. Yan, J. G. Chen, B. Xu, *Angew. Chem. Int. Ed.* **2019**, *58*, 13768–13772.

[27] J. K. Nørskov, J. Rossmeisl, A. Logadottir, L. Lindqvist, J. R. Kitchin, T. Bligaard, H. Jónsson, *J. Phys. Chem. B* **2004**, *108*, 17886–17892.

Graphical TOC
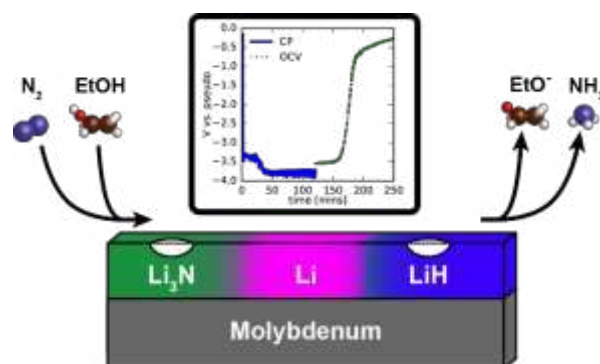
A Dynamic Trio: Electrodeposited lithium is an active electrochemical ammonia synthesis catalyst. Voltammetry and impedance spectroscopy show that the active surface is composed of reduced lithium species. Density Functional Theory shows the activity role for lithium metal, lithium nitride, and lithium hydride.

Keywords

Ammonia, catalysis, density functional calculations, electrochemistry

13